N-myc regulates growth and fiber cell differentiation in lens development

Gabriel R. Cavalheiro[a,1], Gabriel E. Matos-Rodrigues[a], Yilin Zhao[b], Anielle L. Gomes[a],
Deepti Anand[f], Danilo Predes[a], Silmara de Lima[a], Jose G. Abreu[a], Deyou Zheng[b,d,e],
Salil A. Lachke[f,g], Ales Cvekl[b,c], Rodrigo A. P. Martins[a,*]

[a] *Programa de Biologia Celular e do Desenvolvimento, Instituto de Ciências Biomédicas, Universidade Federal do Rio de Janeiro, Rio de Janeiro, RJ, Brazil*
[b] *Department of Genetics, Albert Einstein College of Medicine, Bronx, NY, USA*
[c] *Department of Ophthalmology and Visual Sciences, Albert Einstein College of Medicine, Bronx, NY, USA*
[d] *Department of Neurology, Albert Einstein College of Medicine, Bronx, NY, USA*
[e] *Department of Neuroscience, Albert Einstein College of Medicine, Bronx, NY, USA*
[f] *Department of Biological Sciences, University of Delaware, Newark, DE, USA*
[g] *Center for Bioinformatics and Computational Biology, University of Delaware, Newark, DE, USA*

ARTICLE INFO

ABSTRACT

Myc proto-oncogenes regulate diverse cellular processes during development, but their roles during morphogenesis of specific tissues are not fully understood. We found that *c-myc* regulates cell proliferation in mouse lens development and previous genome-wide studies suggested functional roles for *N-myc* in developing lens. Here, we examined the role of *N-myc* in mouse lens development. Genetic inactivation of *N-myc* in the surface ectoderm or lens vesicle impaired eye and lens growth, while "late" inactivation in lens fibers had no effect. Unexpectedly, defective growth of *N-myc*-deficient lenses was not associated with alterations in lens progenitor cell proliferation or survival. Notably, *N-myc*-deficient lens exhibited a delay in degradation of DNA in terminally differentiating lens fiber cells. RNA-sequencing analysis of *N-myc*-deficient lenses identified a cohort of down-regulated genes associated with fiber cell differentiation that included DNaseIIβ. Further, an integrated analysis of differentially expressed genes in *N-myc*-deficient lens using normal lens expression patterns of *iSyTE*, *N-myc*-binding motif analysis and molecular interaction data from the String database led to the derivation of an *N-myc*-based gene regulatory network in the lens. Finally, analysis of *N-myc* and *c-myc* double-deficient lens demonstrated that these Myc genes cooperate to drive lens growth prior to lens vesicle stage. Together, these findings provide evidence for exclusive and cooperative functions of *Myc* transcription factors in mouse lens development and identify novel mechanisms by which *N-myc* regulates cell differentiation during eye morphogenesis.

1. Introduction

Myc proto-oncogenes are transcriptional regulators of genes involved in multiple cellular processes such as proliferation, metabolism, differentiation and tumorigenesis (Eilers and Eisenman, 2008; Kress et al., 2015). This family of helix-loop-helix (bHLH) transcription factors has three members (*c-myc*, *N-myc* and *L-myc*) that regulate gene expression through distinct mechanisms. Transcriptional activation by Myc proteins depend on heterodimerization with Max and binding to E-box motifs widespread throughout genome followed by recruitment of chromatin remodeling enzymes (Meyer and Penn, 2008). In contrast, transcriptional repression by Myc proteins normally involves interaction of the Myc-Max heterodimer with different partners (e.g. Miz-1) at different genomic binding sites (e.g. Initiator element, Inr). Misexpression of Myc was described in various human tumors, and *N-myc* levels correlate with tumor aggressiveness (Beltran, 2014). Findings that Myc are weak transcriptional activators and that *c-myc* binds to thousands of genomic loci suggested that instead of regulating specific gene programs, *c-myc* would globally modulate chromatin structure and act as an amplifier of transcription (Knoepfler et al., 2006). Interestingly, recent next-generation sequencing studies provided evidence that in the context of tumorigenesis, elevated levels of Myc activate and repress context-specific gene expression profiles (Sabo et al., 2014). However, it is currently unclear

whether all Myc family members function as global regulators of transcription or whether they also contribute to the establishment of specific gene programs at physiological levels (e.g. during development).

In addition to important roles in human cancers, Myc genes play a multitude of roles during embryonic development. In humans, *N-myc* haploinsufficiency leads to Feingold syndrome (OMIM 164280), which is characterized by developmental disorders, including microcephaly and short palpebral fissures (van Bokhoven et al., 2005). Genetic studies in mice have shown that *c-myc* and *N-myc* are crucial for development since targeted inactivation of either gene resulted in embryonic lethality (Charron et al., 1992; Sawai et al., 1993; Stanton et al., 1992). Furthermore, *N-myc* and *c-myc* display non-overlapping embryonic expression patterns, suggesting functional divergence (Harris et al., 1992; Yamada, 1990). Tissue-specific inactivation studies revealed organ-specific functions of both *c-myc* and *N-myc*. Roles of *N-myc* were demonstrated in brain (Knoepfler et al., 2002), lung (Okubo et al., 2005), retina (Martins et al., 2008), hematopoietic stem cells (Laurenti et al., 2008), ear (Dominguez-Frutos et al., 2011), heart (Harmelink et al., 2013), and olfactory development (Wittmann et al., 2014). Even though, these studies did not analyze how *N-myc* regulates global gene expression during morphogenesis, few of these demonstrated functional compensation or redundancy between *Myc* family members. Currently, it remains poorly understood how these genes act in coordination to regulate morphogenesis during development (Wey et al., 2010; Zhou et al., 2011)

The developing lens is an advantageous model to study transcriptional regulation of tissue morphogenesis and underlying gene regulatory networks (GRNs) (Cvekl and Ashery-Padan, 2014). In the mouse, eye development begins at embryonic day 9 (E9), when the optic stalk contacts the head surface ectoderm, inducing the formation of the lens placode. Around E10.5, this placode invaginates and detaches from the ectoderm to form the lens vesicle. FGF and BMP growth factors secreted by the adjacent optic vesicle induce cell cycle exit and differentiation of lens vesicle posterior cells into primary fiber cells. In the lens anterior epithelium, progenitor cells proliferate and migrate towards the equatorial region, where they exit cell cycle and differentiate to form secondary fiber cells (Lovicu and McAvoy, 2005). During the onset of terminal differentiation, fiber cells degrade their nuclei and other organelles to form the organelle free zone (OFZ) to prevent light scattering (Bassnett, 2009; Wride, 2011). Nuclei degradation is crucial for OFZ formation and requires DNaseIIβ (Nishimoto et al., 2003). How genes controlling terminal differentiation and organelle degradation are precisely regulated in lens fiber cells is not fully understood. In addition, because the lens is a relatively less complex tissue with only two cell types it serves as a good model to investigate the distinct and/or overlapping contributions of specific proteins of a gene family.

Previously, we characterized the physiological roles of *c-myc* in mouse lens development (Cavalheiro et al., 2014). Inactivation of *c-myc* in the surface ectoderm impaired lens growth and caused microphthalmia due to decreased cell proliferation. Even though *c-myc* is required for the expansion lens progenitor cells pool, cell survival and differentiation were not affected by *c-myc* loss. *N-myc* is also dynamically expressed in the developing lens of various species (Harris et al., 1992; Yamada, 1990). The *iSyTE* database places *N-myc* within a group of candidate cataract-causing genes (Lachke et al., 2012). *In situ* hybridization data of the Eurexpress database shows that, while *c-myc* is restricted to epithelial cells, *N-myc* mRNA is highly expressed in post-mitotic fiber cells. Consistent with a physiological role for *N-myc* in lens development, deletion of chromatin remodelers *CBP* and *p300* from the surface ectoderm decreased *N-myc* expression and severely impaired lens development (Wolf et al., 2013b). In addition, FGF2-induced differentiation of lens epithelial cells in vitro upregulated *N-myc*, indicating that *N-myc* may play a role in fiber cells (Wolf et al., 2013a).

To examine the roles of *N-myc* in mouse lens development and clarify how *c-myc* and *N-myc* coordinately regulate morphogenesis, we genetically inactivated *N-myc*, as well as *c-myc* and *N-myc* together, using different Cre lines. To identify *N-myc*-dependent regulatory events, we performed global gene expression analysis of a *N-myc*-deficient lens by high-throughput RNA-sequencing. Here, we report that *N-myc* is required for lens growth and terminal differentiation of fiber cells during lens development and suggest that *N-myc* regulates context-specific gene expression profiles in the developing eye.

2. Materials and methods

2.1. Mice

Experimental procedures were approved by the Committee of ethics in animal use (CEUA/CCS/#092/15). Mice carrying *N-myc*[loxP] (MGI: 2388717) (Knoepfler et al., 2002), *c-myc*[loxP] (MGI: 2178233) (de Alboran et al., 2001), α-Cre (Tg(Pax6-cre,GFP)2Pgr) (MGI: 3052661) (Marquardt et al., 2001), Le-Cre (Tg(Pax6-cre,GFP)1Pgr) (MGI: 3045749) (Ashery-Padan et al., 2000), Mlr10-Cre (Tg(Cryaa-cre) 10Mlr) (MGI: 3038243) and Mlr39-Cre (Tg(Cryaa-cre)39Mlr) (MGI: 3811526) (Zhao et al., 2004) were kindly shared. Control group consisted Cre -/- mice with Myc genes flanked by loxP sites: N-myc[loxP/loxP] (*N-myc*[Ctrl]) and N-myc[loxP/loxP];c-myc[loxP/loxP] (*N-myc; c-myc*[Ctrl]). All Cre transgenes were kept in heterozygosity. *N-myc*[Mlr10-Cre] stands for Mlr10-Cre^{+/-}; N-myc[loxP/loxP]. Similar notations were used for other conditional knockouts (cKO) or double-deficient (DKO). Genotyping was performed as previously (Cavalheiro et al., 2014).

2.2. Volume measurements

Eyes were enucleated, the length of axial (x), dorsal-ventral (y) and medial-lateral (z) axis were measured and volume was calculated as previously (Cavalheiro et al., 2014). Lenses dissected in phosphate-buffered saline (PBS) were similarly measured. Pictures of dissected eyes or lenses were taken using a Zeiss stereoscope and an AxioCamERc 5 s camera.

2.3. Histological processing

Embryonic heads or post-natal eyes were dissected in PBS and fixed overnight in 4% paraformaldehyde in PBS followed by cryopreservation in 30% sucrose. Tissues were embedded in O.C.T. for cryoprotection. 10 μm cryosections were obtained in a Leica1850 cryostat. For histology, sections were stained with DAPI or haematoxilin and eosin staining.

2.4. RNA extraction, RNA-Seq and data analysis

Lenses from single animals were isolated in cold PBS, lysed in TRIzol (ThermoFisher cat#15596026) and stored at −80 °C. After genotyping, samples were mixed based on genotypes. Each realtime RT-PCR sample consisted of a pool of at least 4 lenses. After pooling, chloroform was added and samples were centrifuged at 15,000*g* at 4 °C for 15 min. A mix of the aqueous phase with EtOH (1.5 vol) was processed in RNeasy minicolumns (Qiagen cat#74104). Genomic DNA contamination was verified by PCR. Contaminated samples were treated with DNase I (Ambion cat#1906).

RNA samples with RIN number (Agilent 2100 Bioanalyzer) over 8.0 were used for library construction and 100 bp paired-end sequencing on IlluminaHiSeq. 2500. Around 30 million reads for each sample were obtained. After trimming adapter with Trim Galore (v.0.3.7), RNA-Seq reads were aligned back to the mouse genome (v.mm10) with tophat (v.2.0.13) (Trapnell et al., 2009). Count numbers were calculated with HTseq (v.0.6.1) (Anders et al., 2015) using mm10 (Pruitt et al., 2012) gene annotation file downloaded from UCSC genome browser

(Meyer et al., 2013). The Cufflinks (v.2.2.1) (Trapnell et al., 2010) was then used to calculate FPKM values of the genes. We further focused on 12,370 genes that have mean FPKM value > 1 from all samples. DESeq. 2 (Love et al., 2014) was used to determine differentially expressed genes (GEO #: GSE94061).

The cutoffs for differentially expressed genes (DEGs) were set to log2(fold change) ± > 0.5 with adjusted p value < 0.05 (by Benjamini-Hochberg correction). The gene ontology (GO) functional annotation was performed using the NIH web-based DAVID software (Huang da et al., 2009). To score epithelial- and fiber-cell enrichment of the set of DE genes in *N-myc*$^{Mlr10-Cre}$, we obtained fiber/epithelium enrichment data from a previous study (Hoang et al., 2014).

2.5. iSyTE based lens expression analysis of DEGs

Expression of *N-myc* and *c-myc* in developing lens was analyzed in *iSyTE* database (Lachke et al., 2012) and in isolated lens epithelium (Epi) and fiber cell (FC) datasets at P0 stage (SRP040480) (Hoang et al., 2014). Normal expression profiles of *N-myc*-deficient lens DEGs (RNA-Seq) were also examined using the same datasets. Lens expression scores were computed at embryonic and postnatal stages (E10.5, E11.5, E12.5, E16.5, E17.5, P0, P2, P56) by analyzing published microarray data (GEO: GSE32334, GSE47694, GSE16533, GSE9711) using the whole embryo body (WB)-based *in silico* subtraction approach (Anand et al., 2015; Lachke et al., 2012) chi-square (χ^2) test for goodness of fit followed by a two-tailed *t*-test was used to estimate the significance of the differences in the up- or down-DEGs comparisons to *iSyTE* lens-enrichment.

2.6. Derivation of N-myc-based gene regulatory network in the lens

An integrated analysis using multiple datasets was performed to assemble an N-myc-based gene regulatory network in the lens. First, the N-myc binding E-box motif (MA0104.3), obtained from the motif database *MotifDb* (http://bioconductor.org), was searched 2500 bp upstream of the transcription start site (TSS) of all the DEGs for which the upstream region could be retrieved from the ENSEMBL database. The analysis was carried out in "R" statistical environment (http://www.r-project.org). To derive further molecular connections between the DEGs, protein-protein interaction (PPI) data were extracted from the String database (http://string-db.org) using an in-house *Python* script. These DEGs were also analyzed for their enrichment in isolated lens epithelium and fiber cell at P0. The combined interactions for DEGs obtained from motif binding, PPI and expression in lens epithelium and fiber cells were then integrated using in-house *Python* script and visualized in Cytoscape (www.cytoscape.org).

2.7. Realtime RT-PCR

cDNA was synthesized using the High capacity Kit (ThermoFisher, cat#4368814). Realtime RT-PCR was performed using TaqMan® or Sybr Green® methods in an Applied Biosystems ABI7500. For primers and methodology see Table S1. Data analysis and normalization were performed as described (Cavalheiro et al., 2014). β-actin was used as normalizer of gene expression across development since it varied less than GAPDH in different developmental stages. GAPDH varied less between control and *N-myc*-deficient lens and was used for normalization between genotype groups.

2.8. Immunostaining and TUNEL assay

Immunostaining protocols for each antibody are listed on Table S2. To detect apoptotic cells, the click-it TUNEL® kit (ThermoFisher cat#C10245) was used. Fluorescent images were captured with a Leica TCS-SP5 with an AOBS system and bright field pictures in a Leica DM750.

2.9. Western blotting

Lens were isolated in cold PBS, lysed in RIPA buffer containing protease and phosphatase inhibitors (Table S3) and stored at −80 °C. Based on genotypes, samples were mixed (at least 6 lenses per sample) and measured by Bradford assay. Protein (25 µg) were resolved in acrylamide gels and transfered to nitrocellulose membrane. Table S3 shows blotting conditions. Luminata reagent (Millipore, cat#WBLUF0100) was used for chemiluminescence detection in a BioRad ChemiDoc MP.

2.10. Optomotor response test

Cerebral Mechanics Optometry® system was used following a published protocol (Prusky et al., 2004). Visual accuracy threshold was determined by systematic increments of the spatial frequency until the animal no longer responded. The experimenter was blind in relation to mice genotypes.

2.11. Luciferase reporter assays

Mouse lens epithelial αTN4 cells (Yang and Cvekl, 2005) were cultured in DMEM-F12 medium supplemented with 10% FBS. 4×10^3 cells/well were plated (96-well plate) and cultured for 40 h. Using Lipofectamine 3000, pUB, pUB-N-myc, pkw10 or pwk10-Pax6 plasmids were co-transfected with 100 ng DNaseIIβ-luc (He et al., 2016) and 10 ng CMV-*Renilla* (Promega). Thirty hours after transfection Firefly and *Renilla* luciferase activity were measured using Dual luciferase reporter assay system (Promega). In each well DNaseIIβ-luc reporter firefly luciferase activity was normalized to its CMV-*Renilla* luciferase internal control activity. Three independent repeats in triplicate were performed.

2.12. Statistical analysis

One- or two-way ANOVA or *t*-tests, as well as the corresponding post-tests, were performed. P-values are based on two-sided tests. Analyses were performed with GraphPad Prism.

3. Results

3.1. N-myc expression is enriched in developing lens and is required for lens growth

To comparatively characterize the dynamics of *Myc* genes expression in mouse developing lens, we first analyzed the *iSyTE* database. *N-myc* mRNA expression is higher as compared to *c-myc*, and *N-myc* is lens-enriched from E11.5 through P0 (Fig. 1A). RT-PCR analysis confirmed that *N-myc* is highly expressed during lens embryogenesis and decreases throughout lens maturation (Fig. 1B). To identify the cell populations expressing Myc, a RNA-Seq dataset of isolated P0 lens fiber and epithelial cells was analyzed (Hoang et al., 2014). *N-myc* is expressed at significantly higher levels in fiber cells, while *c-myc* is higher in epithelial cells (Fig. 1C). Immunohistochemistry (IHC) in lens cryosections confirmed that N-myc protein is higher in the nucleus of differentiating lens fiber cells at E12.5 and E14.5 (Fig. 1D).

To inactivate *N-myc* in distinct stages and cell populations of the developing lens, we used 3 distinct mouse Cre lines. In the Le-Cre line, Cre-mediated recombination starts in the lens surface ectoderm at E9.5 (Ashery-Padan et al., 2000). In the Mlr10-Cre, recombinase activity is first detected in the lens vesicle at E10.5 and in the Mlr39-Cre line, Cre activity starts around E12.5, exclusively in lens fibers (Zhao et al., 2004). These Cre lines were used to generate *N-myc*$^{Le-Cre}$, *N-myc*$^{Mlr10-Cre}$ or *N-myc*$^{Mlr39-Cre}$ mice. RT-PCR analysis confirmed that *N-myc* mRNA was reduced in both *N-myc*$^{Le-Cre}$ and *N-myc*$^{Mlr10-Cre}$ lenses (Fig. 1E). Consistently, N-myc IHC signal was
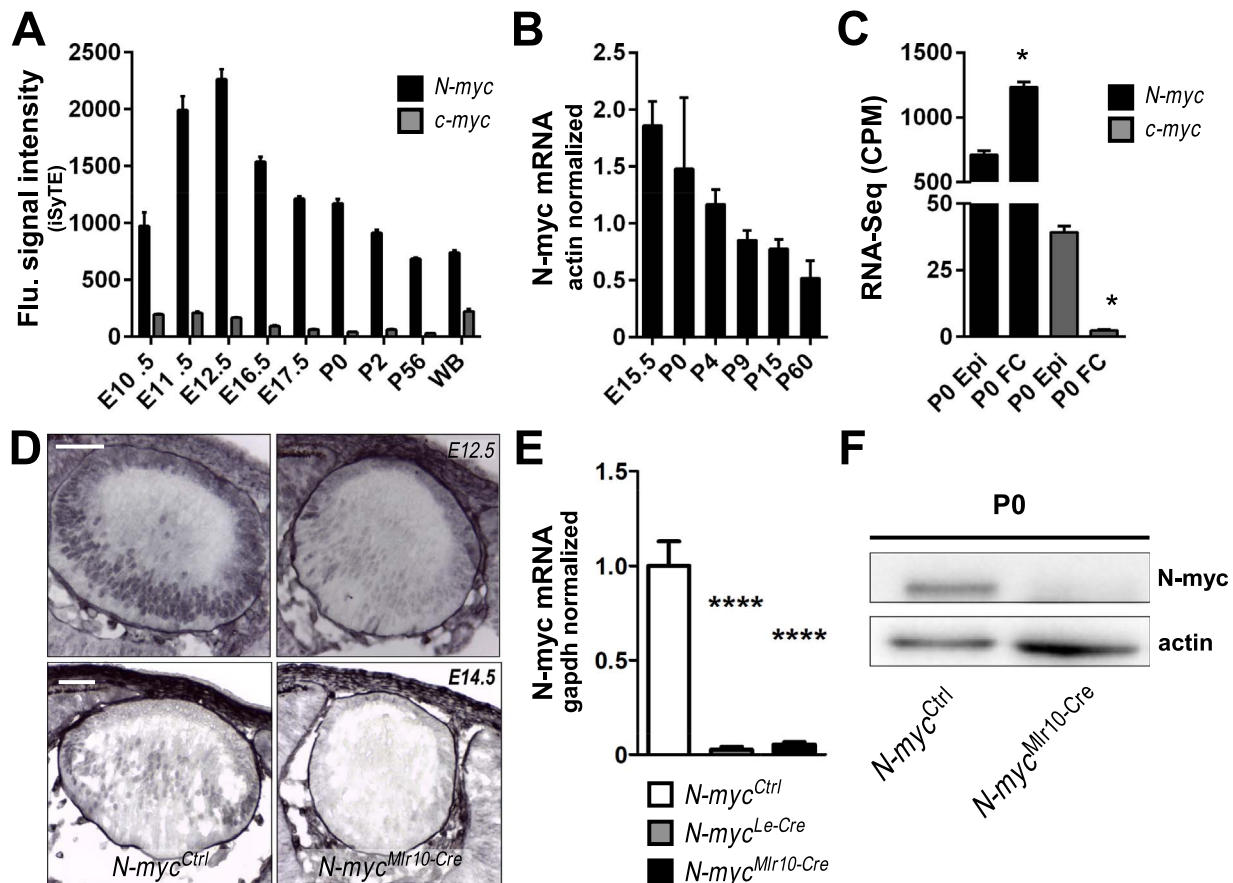
Fig. 1. *N-myc* expression is enriched in the developing mouse lens. (A) *iSyTE* based expression of *N-myc* and *c-myc* mRNA in mouse lens at indicated embryonic and postnatal stages. (B) Realtime RT-PCR of *N-myc* mRNA in various stages of lens development (n = 3). *Actb* TaqMan probes were used to normalize. **(C)** *N-myc* and *c-myc* mRNA content in isolated lens epithelia or fiber cells at P0 (RNA-Seq analysis). **(D)** Immunohistochemistry for N-myc protein (purple) in cryosections of E12.5 and E14.5 lenses. No counterstaining was performed. **(E)** *N-myc* mRNA content (realtime RT-PCR) in P0 *N-myc*[Ctrl] (n = 6), *N-myc*[Le-Cre] (n = 3) and *N-myc*[Mlr10-Cre] (n = 3) lenses. GAPDH was used to normalize. **(F)** Representative western blot analysis of *N-myc* in P0 *N-myc*[Ctrl] and *N-myc*[Mlr10-Cre] lenses (actin was used as loading control) (n = 3). One-way ANOVA with Tukey's posttest performed in C. Error bars indicate S.E.M. in **A** and **C** and S.D. in **B** and **E**; *$p < 0.05$, **** $p < 0.0001$. Scale bar: 50 µm. (WB: whole body reference; CPM: counts per million; Epi: lens epithelial cells; FC: lens fiber cells).

decreased in *N-myc*[Mlr10-Cre] lenses ([Fig. 1](#)D) and western blot revealed a reduction of N-myc protein content ([Fig. 1](#)F).

Le-Cre-mediated inactivation of *N-myc* (*N-myc*[Le-Cre]) reduced the lens and eye volume of adult and postnatal mice ([Fig. 2](#)A-C). However, in our hands, the Le-Cre transgene alone (Le-Cre^{+/-}; N-myc^{+/+} mice) induced apoptosis in E12.5 lenses. In contrast, in Mlr10-Cre^{+/-}; N-myc^{+/+} mice, no evidence of Cre effects was observed (data not shown). To confirm the relevance of *N-myc* to eye growth, we measured lens and eye volume of *N-myc*[Mlr10-Cre] mice. Mlr10-Cre-mediated inactivation of *N-myc* also induced eye and lens volume reduction ([Fig. 2](#)A-C). In *N-myc*[Mlr10-Cre] mice, eye growth impairment was already detectable at P0, indicating that *N-myc* contributes for lens growth during embryogenesis ([Fig. 2](#)B). When *N-myc* was inactivated specifically in lens fiber cells (*N-myc*[Mlr39-Cre]) growth was not affected ([Fig. S1](#)A-B). Next, we tested whether the observed defects affected visual acuity. Behavioral optomotor response was not compromised in *N-myc*[Mlr10-Cre] adult mice ([Fig. 2](#)D). These data indicate that *N-myc* function in the lens is required for lens and eye growth during development.

Previously, we showed that inactivation of *N-myc* in developing retina and lens impaired eye, retina and lens growth ([Martins et al., 2008](#)) and proposed that defective retinal growth affected lens formation. To further investigate this model, we used α-Cre to inactivate *N-myc* only from the retinal progenitor cells (RPC) (*N-myc*[α-Cre]). Consistent with a role of *N-myc* in RPCs, the retinal volume was reduced in *N-myc*[α-Cre] mice ([Fig. S1](#)C). However, in contrast to concomitant *N-myc*-inactivation in the retina and lens (*N-myc*[Nes-Cre]), *N-myc* loss only in RPCs did not affect lens and eye volume ([Fig. S1](#)A-B).

3.2. N-myc is required for growth and terminal differentiation during embryogenesis

To further elucidate how *N-myc* inactivation affected lens development, we analyzed the histology of *N-myc*[Mlr10-Cre] embryonic lenses. At E12.5, no histological differences were apparent between *N-myc*-deficient and control lenses ([Fig. 2](#)E). However, at E17.5, in addition to a reduction in size ([Fig. 2](#)F), a central region devoid of nuclei was not distinguishable in *N-myc*[Mlr10-Cre] lens, ([Fig. 2](#)G and g′). Interestingly, nuclei in lens central region persisted until P0 ([Fig. 6](#)), but were not observed at P7 ([Fig. 2](#)H). At P60, *N-myc*[Mlr10-Cre] lenses were transparent ([Fig. 2](#)I).

Consistent with the earlier onset of Cre activity, in *N-myc*[Le-Cre] lens size was reduced earlier than in *N-myc*[Mlr10-Cre] mice. At E13.5, *N-myc*[Le-Cre] lens were smaller than control littermates ([Fig. S1](#)D-G). *N-myc*[Le-Cre] lenses also displayed nuclei in lens central region at E17.5 and P0 ([Fig. 6](#)B-E).

3.3. N-myc inactivation did not affect cell proliferation or survival in the developing lens

We found that c-*myc* drives cell proliferation during lens embryogenesis ([Cavalheiro et al., 2014](#)) and *N-myc* is a known regulator of cell proliferation in various tissues ([Dominguez-Frutos et al., 2011](#); [Knoepfler et al., 2002](#); [Martins et al., 2008](#); [Okubo et al., 2005](#)). We tested whether inactivation of *N-myc* would be associated with cell proliferation defects by staining and scoring the proportion of
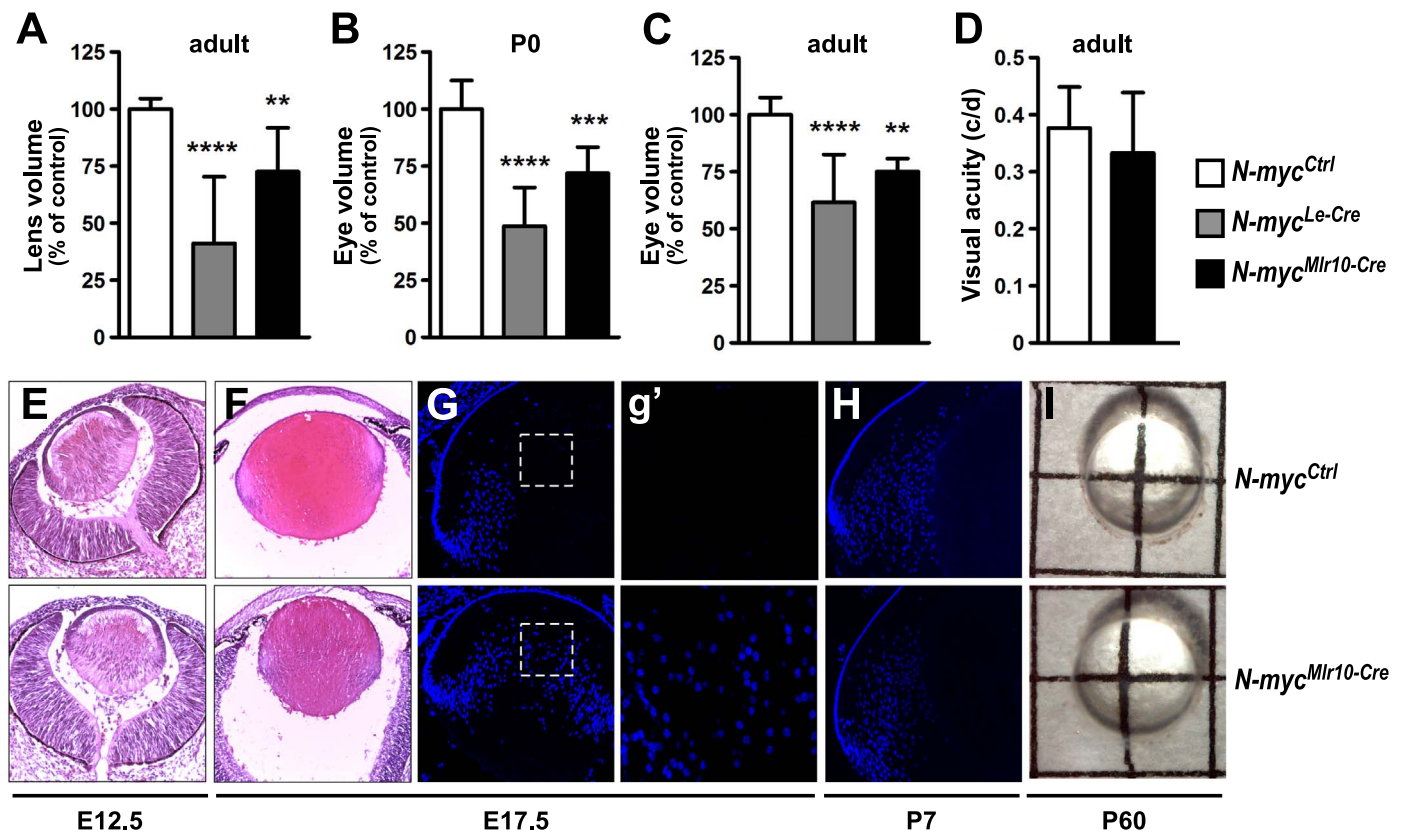
Fig. 2. *N-myc* inactivation in the lens impair eye and lens growth. **(A-C)** Measurements of lens volume (adult) and eye volume (P0 and adult) in *N-myc*[Ctrl] (n = 9), *N-myc*[Mlr10-Cre] (n = 5), *N-myc*[Le-Cre] (n = 6) (control = 100%). **(D)** Visual acuity by optomotor response test in adult (P60) *N-myc*[Ctrl] (n = 12) and *N-myc*[Mlr10-Cre] (n = 13) mice. **(E-F)** Representative pictures of haematoxilin & eosin stainings of E12.5 and E17.5 lenses. **(G-H)** Representative pictures of DAPI nuclear staining of E17.5 and P7 lenses. **(g')** Insets from (G) reveal the absence or presence of nuclei in the center of the E17.5 control and *N-myc*-deficient lenses. **(I)** Representative pictures of isolated lenses from P60 mice. One-way ANOVA with Tukey's posttest performed in A-C and a *t*-test in D. Error bars indicate S.D.; **p < 0.01, *** p < 0.001, ****p < 0.0001. Scale bar: 100 µm.

various markers of cell proliferation in different stages of lens development.

First, we scored the proportion of phospho-histone H3 immunopositive epithelial cells (pH3+), a marker of cells in G2/M, in *N-myc*[Mlr10-Cre] and control lens at E12.5 and E14.5. No difference in the proportion of pH3+ cells was observed (Fig. 3A-C). The proportion of BrdU+ and PCNA+ cells was also not altered at E12.5, E14.5 (BrdU+, Fig. 3G) or P0 (PCNA+, Fig. 3H) in *N-myc*[Mlr10-Cre] lens. Consistently, *N-myc* inactivation in the lens placode (*N-myc*[Le-Cre]) did not affect cell proliferation levels at E13.5, E17.5 or P0 (PCNA+ or pH3+) (Fig. S1H-K). These data suggest that *N-myc* does not regulate cell proliferation in developing lens.

To test whether *N-myc* inactivation could increase cell death during lens development, we performed TUNEL assays. We did not observe any increase in the proportion of TUNEL+ cells in *N-myc*-deficient lenses in the stages analyzed (Fig. 3D-F). Collectively, these findings indicate that the cell cycle and cell survival regulation occur normally in the absence of *N-myc* during embryonic stages of lens development.

3.4. N-myc and c-myc functionally cooperate during lens development

Loss of either *N-myc* or *c-myc* impaired lens growth, but cell proliferation defects were exclusively observed in *c-myc*-deficient lens (Cavalheiro et al., 2014). Considering previous reports of cross-regulation of *Myc* family members, we hypothesized that *c-myc* could compensate for *N-myc* loss to maintain normal cell proliferation in *N-myc*-deficient lenses. Other non-excluding possibility is that *N-myc* and *c-myc* may play distinct roles to promote lens growth.

First, we measured the mRNA levels of other Myc family members in *N-myc*-deficient lenses and observed an increase in *c-myc* mRNA

content in *N-myc*[Mlr10-Cre] lenses at P0 (Fig. 4A). In *N-myc*[Le-Cre] lenses, a similar increase in *c-myc* and an increase in *L-myc* mRNA levels was also detected (Fig. S2A-B), indicating that the expression of other *Myc* genes is upregulated upon *N-myc* loss in the lens.

To evaluate whether Myc proto-oncogenes act in concert to regulate lens development, we inactivated *N-myc* and *c-myc* simultaneously in the lens vesicle (*N-myc; c-myc*[Mlr10-Cre]) or in the surface ectoderm (*N-myc; c-myc*[Le-Cre]). No major histological differences between single or double-deficient embryonic lenses were observed (Fig. 4B-D). Consistently, lens and eyes of *N-myc; c-myc*[Mlr10-Cre] and *N-myc*[Mlr10-Cre] mice had similar size at P0 and P60 (Fig. 4E-F). Besides growth defects, eyes from *N-myc; c-myc*[Mlr10-Cre] mice also exhibited anterior segment defects (evident pigmented material) (Fig. 4G-H), a phenotype previously observed following *c-myc*-inactivation in the surface ectoderm (Cavalheiro et al., 2014).

To better understand the cellular basis of the DKO lens/eye growth impairment, we performed immunolabeling for cell proliferation markers. Consistent with the defective cell proliferation of *c-myc*-deficient lenses, we detected a decrease in the proportion of pH3+ epithelial cells soon after *N-myc* and *c-myc* inactivation (E12.5) (*N-myc;c-myc*[Ctrl] = 3.06 ± 0.9% vs. *N-myc; c-myc*[Mlr10-Cre] = 1.36 ± 0.9%) (Fig. 4I-K). However, the proportion of both PCNA+ and BrdU+ epithelial cells was not altered in double-deficient lenses throughout embryonic development (Fig. 4L-M). *N-myc* and *c-myc* were shown to cooperatively regulate the survival of hematopoietic progenitor cells (Laurenti et al., 2008). However, the proportion of cleaved-caspase-3+ cells was not altered upon Mlr10-Cre-mediated loss of both *N-myc* and *c-myc* (Fig. 4N), suggesting that during lens embryogenesis *Myc* genes do not regulate cell survival.
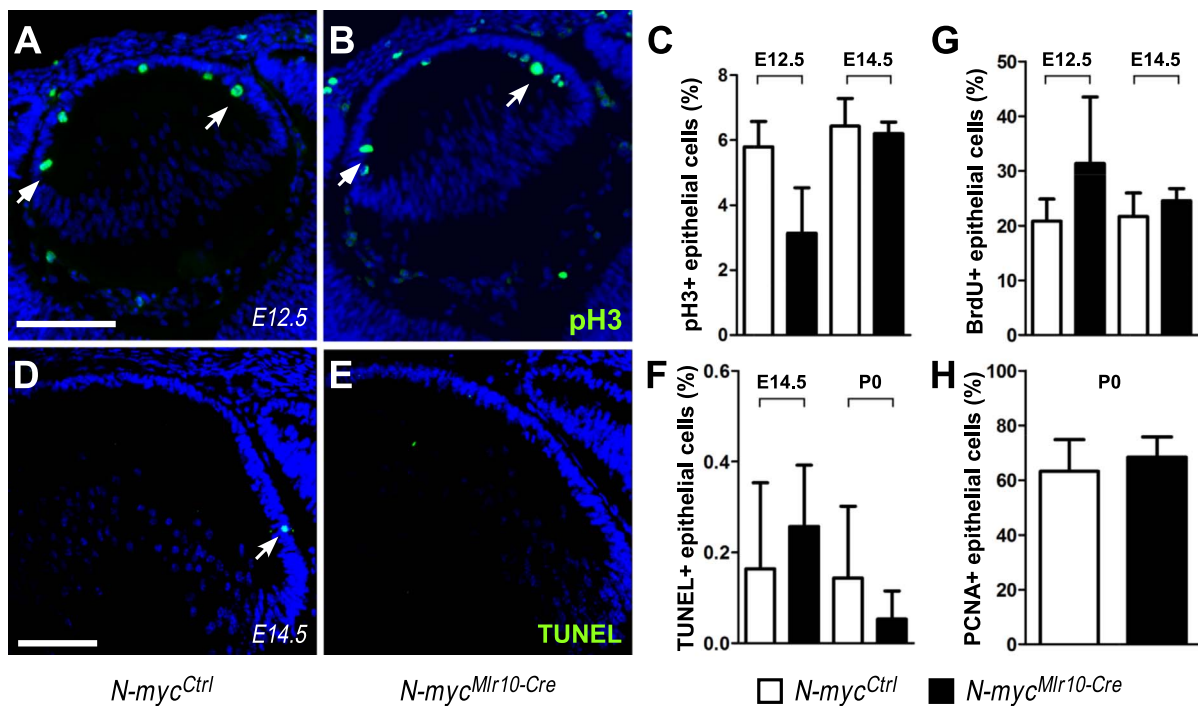
Fig. 3. *N-myc*-inactivation did not affect cell proliferation or cell survival in developing lens. **(A-B)** Representative pictures of pH3 immunostaining in *N-myc*[Ctrl] and *N-myc*[Mlr10-Cre] lenses at E12.5. **(C)** Proportion of pH3+ epithelial cells at E12.5 (n = 3) and E14.5 (n = 3). **(D-E)** Representative pictures of TUNEL staining in *N-myc*[Ctrl] and *N-myc*[Mlr10-Cre] lenses at E14.5 **(F)** Proportion of TUNEL+ cells in E14.5 (n = 4) and P0 (n = 3) lenses. **(G-H)** Quantification of BrdU+ (n = 4) and PCNA+ (n = 8) epithelial cells in the indicated developmental stages. *t*-tests were performed to compare *N-myc*[Ctrl] and *N-myc*[Mlr10-Cre] in every graph. Error bars indicate S.D.; Scale bar: 100 μm.

Interestingly, in comparison to single *N-myc* inactivation (*N-myc*[Le-Cre]), double inactivation of *N-myc* and *c-myc* at the lens placode stage (*N-myc; c-myc*[Le-Cre]) led to a severe growth impairment after birth (Fig. S2C). Histology of E13.5 *N-myc; c-myc*[Le-Cre] lens showed that this striking growth defect started early during embryogenesis (Fig. S2D-F). The finding that *c-myc* inactivation in *N-myc*-deficient lens placode led to an additive phenotype already at E13.5 suggests that before lens vesicle formation *N-myc* and *c-myc* may either compensate each other loss or act through different pathways to stimulate lens growth.

3.5. N-myc regulates the transcription of genes involved in lens differentiation

Myc transcription factors regulate the expression of genes involved in basal cellular processes such as transcription and translation as well as genes with tissue-specific function (Kress et al., 2015). Most investigations on global regulation of gene expression by *N-myc* evaluated its gain of function (Berwanger et al., 2002; Dardenne et al., 2016; Poschl et al., 2014), therefore it is not clear whether *N-myc* regulate tissue-specific targets during embryonic development. To understand the consequences of *N-myc* loss to the developing lens transcriptome, we performed RNA-Seq comparing E14.5 *N-myc*[Mlr10-Cre] and *N-myc*[Ctrl] lenses. Using a cutoff of log2(fold change) > 0.5 and < −0.5, and an adjusted p-value of 0.05, we detected 483 down- and 659 upregulated genes in *N-myc*-deficient lenses (Fig. S3, Tables S4 and S5). A gene ontology (GO) analysis revealed that the represented categories for upregulated genes in *N-myc*[Mlr10-Cre] lenses included cell adhesion and glycoproteins, while the represented classes of down-regulated genes were related to control of translation and protein folding (Fig. S3, Tables S4 and S5). These findings corroborate previous studies showing that *N-myc* regulates basal cellular processes and suggest that a global reduction in regulators of protein synthesis may contribute to the lens growth phenotypes of *N-myc*-deficient lenses.

To estimate whether some of the differentially expressed genes (DEGs) may represent potential direct targets of *N-myc*, we performed a search for E-box binding motifs in the 2500 bp upstream genomic regions of the transcription start site (TSS) of all the DEGs containing such regions in the ENSEMBL database. Approximately, 35% of the upregulated and downregulated DEGs have at least one potential N-myc binding motif (Fig. S4 and Table S6).

To specifically address the importance of *N-myc* for the expression of genes crucial for lens development and provide additional insights about the normal dynamics of the DEGs, a comparative analysis of E10.5, E12.5 and E16.5 *iSyTE* lens enrichment scores and *N-myc* cKO DEGs was performed (Fig. 5A). The number of lens-enriched genes that were downregulated following *N-myc* loss progressively increased from E12.5 to E16.5 (numbers in upper left quadrants). In contrast, the majority of *N-myc* cKO up-regulated genes were not lens enriched (numbers in bottom right quadrants) (Fig. 5A). These data indicate that *N-myc* loss results in downregulation of genes that are normally enriched in the lens as it progress from E12.5 to E16.5, suggesting that *N-myc* may be important to induce the expression of genes enriched in differentiating fiber cells and to repress genes that are not enriched in the lens.

Consistent with the higher expression of *N-myc* in lens fiber cells (Fig. 1C-D) and the transient impairment of fiber cell denuclation following *N-myc* loss (Fig. 2F-G), several genes with described roles in lens differentiation were misregulated in *N-myc*[Mlr10-Cre]. *DNaseIIβ* (second most downregulated gene), *Birc7*, *Capn3*, *Gje1* and *Hopx,* which are expressed in late stages of fiber cell differentiation, were downregulated in *N-myc*-deficient lenses. Similarly, we detected down-regulation of RNA-binding proteins (*Caprin2* and *Tdrd7*) (Dash et al., 2015; Lachke et al., 2011), regulators of autophagy (*Gabarapl1* and *Park7*) (Sun et al., 2015), and components of cytoskeleton systems (*Bfsp1* and *Tmod1*) (Perng et al., 2007; Gokhin et al., 2012) that are highly expressed by fiber cells (Fig. 5B, Fig. S5 and Table S5). Interestingly, many of these contained N-myc binding motifs in their promoter regions (Fig. S4 and Table S6).

To compare the relevance of *N-myc* for the transcriptome of specific compartments of the developing lens (progenitor vs. differentiating cells), we retrieved genes whose expression is greater (or enriched) in
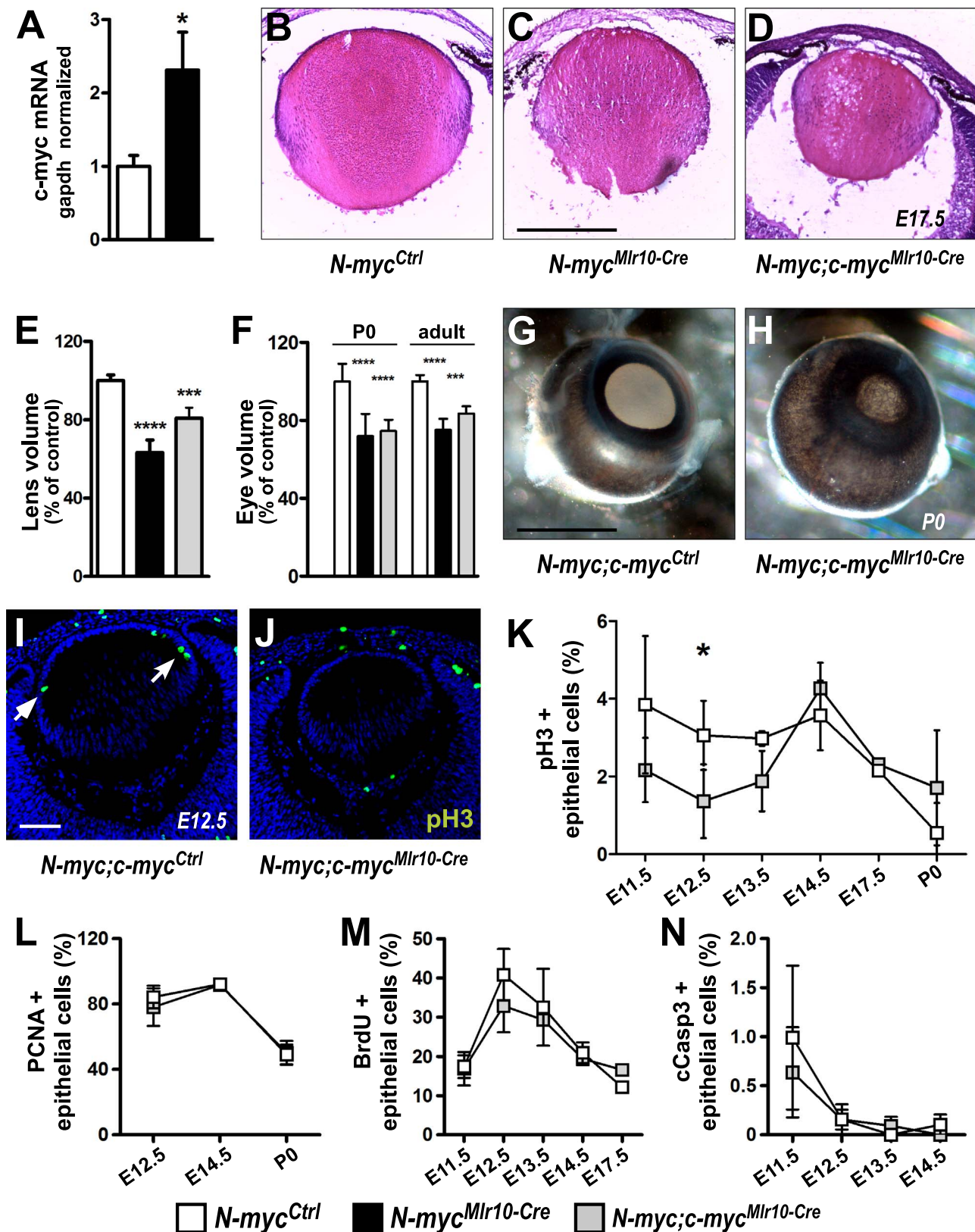
Fig. 4. Simultaneous *N-myc* and *c-myc* inactivation after lens vesicle stage. (A) Realtime RT-PCR analysis of *c-myc* mRNA content in *N-myc*[Ctrl] and *N-myc*[Mlr10-Cre] lenses at P0 using *c-myc* and *Gapdh* TaqMan probes (n = 3). **(B-D)** Representative pictures of H & E stained *N-myc;c-myc*[Ctrl], *N-myc*[Mlr10-Cre] and *N-myc;c-myc*[Mlr10-Cre] lens at E17.5. **(E-F)** Volume measurements of *N-myc;c-myc*[Ctrl], *N-myc*[Mlr10-Cre] and *N-myc;c-myc*[Mlr10-Cre] lens (P60, n = 4) and eyes (P0, n = 5 and adult, n = 4). **(G-H)** Representative pictures of *N-myc;c-myc*[Ctrl] and *N-myc;c-myc*[Mlr10-Cre] P0 eyes. **(I-J)** Representative pictures of pH3 immunostaining of *N-myc;c-myc*[Ctrl] and *N-myc;c-myc*[Mlr10-Cre] E12.5 lenses (arrows indicate pH3+ cells). **(K-N)** Proportion of pH3+ (K), PCNA+ (L), BrdU+ (M), and cleaved-caspase-3+ (N) lens epithelial cells in *N-myc;c-myc*[Ctrl] and *N-myc;c-myc*[Mlr10-Cre] in different developmental stages (n = 3). *t*-tests performed in A,K and N. One-way ANOVA with Tukey's posttest performed in E and F. Error bars indicate S.D.; *$p < 0.05$, *** $p < 0.001$, ****$p < 0.0001$. Scale bar: 100 μm.
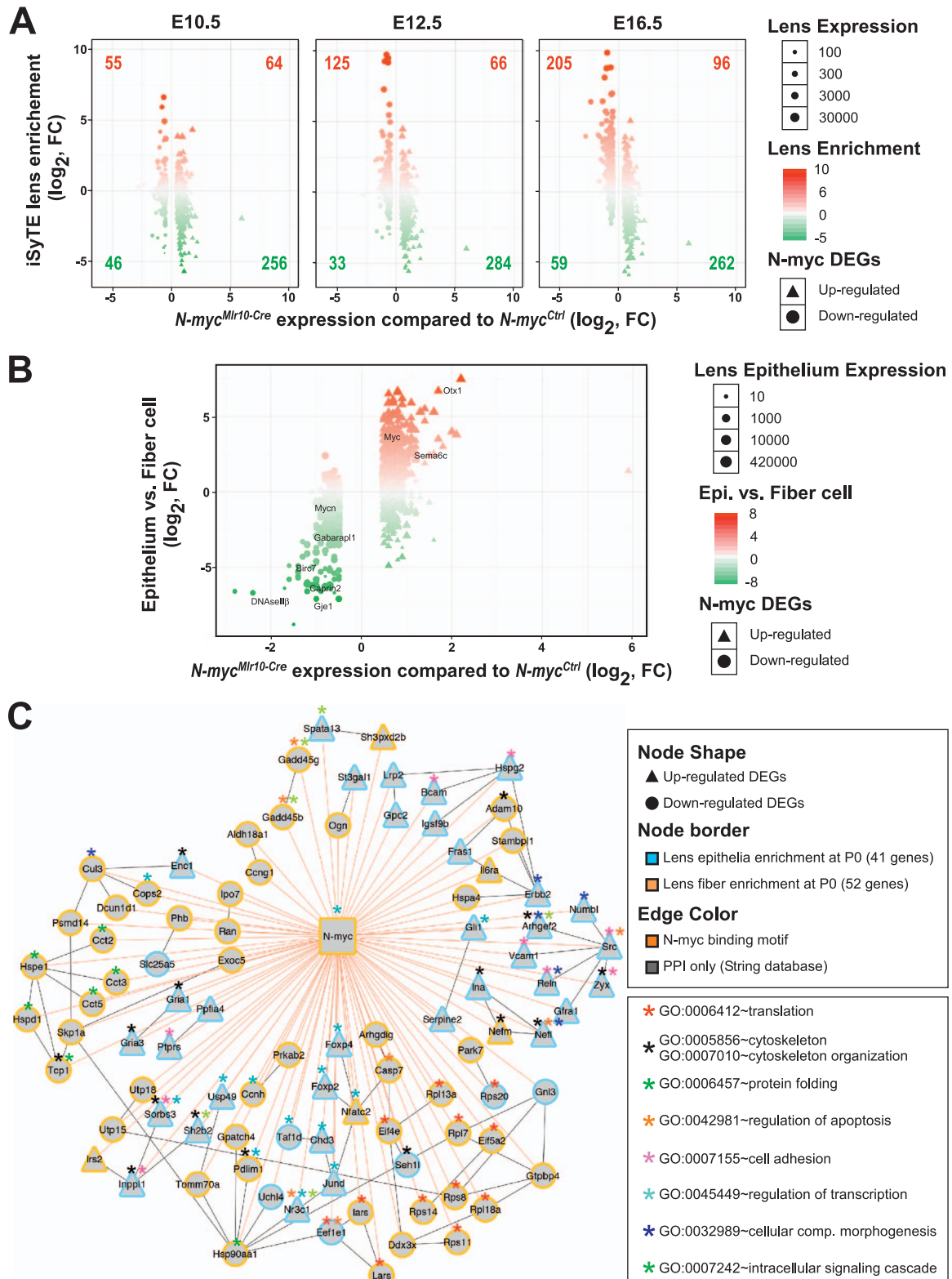
Fig. 5. Transcriptome of *N-myc*-deficient lens reveals changes in gene expression in epithelial and fiber cells. (A) The *iSyTE* lens-enrichment score (y-axis) for down- and up-regulated *N-myc*-deficient lens DEGs (x-axis) was computed by comparing lens expression with the whole embryo body (WB) reference control at embryonic stages E10.5, E12.5 and E16.5. Circles represent down-regulated and triangles represent upregulated DEGs in *N-myc*-deficient. Lens-enrichment scores are indicated by colors: Red represents lens-enriched genes and green represents genes expressed at higher levels in the WB reference. Lens expression levels in *iSyTE* are indicated by the size of circles and triangles. As the lens progresses from E10.5 to E12.5, majority of down- and up-regulated DEGs fall into the lens-enriched (upper left and right quadrant). The difference between lens enriched DEGs compared to lens non-enriched DEGs was significant for E12.5 and E16.5. A χ^2 test for goodness of fit ($p < 0.00001$) and a two-tailed *t*-test were performed. **(B)** *N-myc*-deficient lens DEGs (x-axis) were plotted against previously identified epithelial- or fiber-enriched genes in P0 mouse lens (y-axis; fiber enrichment is negative). **(C)** A N-myc-regulatory network was assembled based in the integration of multiple data (presence of N-myc binding motifs in DEGs, known protein-protein interactions between DEGs, overlay of information on enriched GO categories). *N-myc*-deficient lens DEGs (57 down-regulated circles and 33 up-regulated triangles) identifed with putative N-myc binding motifs in their 2500 bp upstream of TSS (edge color = orange) were subjected to String database analysis to compute evidence from molecular interaction with edge score > 400 (edge color = grey). DEGs were also analyzed for enrichment in isolated lens epithelium (Epi) and fiber cell (FC) at P0 (blue node border represents Epi-enriched and yellow node border represents FC-enriched). Asterisk indicates enriched GO categories identified in the network.

epithelial or fiber cells (Hoang et al., 2014) and crossed them with the *N-myc*-deficient lens DEGs. Notably, using a cutoff of ≥ 0.5 (log2), ~78% (379/483) of the genes downregulated in *N-myc*[Mlr10-Cre] lenses were fiber-enriched, while only ~ 11% (51/483) showed epithelial enriched expression (Fig. 5D). Of upregulated genes in *N-myc*[Mlr10-Cre] lenses, ~ 20% (132/659) were fiber-enriched genes, while ~ 61% (399/659) presented epithelial enrichment (Fig. 5D), suggesting that *N-myc* is important for the transcriptional activation of a relevant subset of fiber-enriched genes and also for the repression of some epithelia-enriched genes during lens differentiation. Thus, *N-myc* is required to drive expression of various genes important for fiber cell differentiation.

3.6. N-myc is required for correct timing of nuclear degradation during lens terminal differentiation

Given the downregulation of fiber-cell genes following *N-myc* loss, we asked if *N-myc* would be required for the early steps of fiber cell formation, and therefore indirectly regulate denucleation. During early fiber cell differentiation, Erk1/2 are activated by FGF signaling (Audette et al., 2016; Zhao et al., 2008). Immunofluorescence analysis at E13.5 revealed no alteration in Prox1, c-Maf or pERK1/2 (phosphorylated ERK1/2) (Fig. S7) in *N-myc*[Le-Cre]. Consistent with the minor alterations in the cell cycle of *N-myc*-deficient lenses, no alterations in Foxe3, p27[Kip1] cyclin D1 or cyclin D2 expression patterns were observed at E13.5 (Fig. S7). Together with the transcriptome data, these results suggest that *N-myc* does not control the expression of either cell cycle modulators or known transcriptional regulators of early fiber cell differentiation.

Because *N-myc*[Mlr10-Cre] and *N-myc*[Le-Cre] mice exhibited remnant nuclei in their lenses, the process of DNA degradation was analyzed in *N-myc*-deficient lenses by performing immunofluorescence for γH2AX, a marker of DNA double-strand breaks. In control lens, γH2AX+ fiber cells were detected in the center of the control lens at E17.5 (Fig. 6A) and P0 (Fig. 6D). In *N-myc*-deficient lens (*N-myc*[Mlr10-Cre] and *N-myc*[Le-Cre]), no γH2AX+ cells were observed at E17.5 (Fig. 6B-C). Later, in P0, few γH2AX+ cells with a disorganized spatial pattern were identified in cKO lenses that did not present a nuclei-free region (Fig. 6E-F). The overdue detection of γH2AX+ cells at P0 is consistent with the delayed denucleation of *N-myc*-deficient lenses.

3.7. Molecular changes associated to defective denucleation in N-myc-inactivated lenses

The downregulation of *DNaseIIβ* at E14.5 and the absence of γH2AX in primary fiber cell nuclei of *N-myc*-deficient lens at E17.5, prompted us to investigate whether the *N-myc* loss would affect nuclear DNA accessibility and/or *DNaseIIβ* expression. p27[Kip1] and Cdk1 are important for the disassembly of nuclei envelope and lens DNA degradation (Chaffee et al., 2014; Lyu et al., 2016; Rowan et al., 2016). During fiber cells differentiation the levels of p27[Kip1] protein decreases and becomes undetectable prior to nuclear disassembly. In control E17.5 lens, a sharp boundary in the center of the lens marks disappearance of p27[Kip1] signal, while in the *N-myc*[Mlr10-Cre] lens the remnant nuclei in the center of lenses continue to express low levels p27[Kip1] (Fig. 7A-D).

Downregulation of p27[Kip1] is necessary for Cdk1 activity in late fiber cells and inactivation of this kinase completely abrogates phosphorylation of its target NuMA (Chaffee et al., 2014). To provide evidence of whether Cdk1 activity would be impaired in *N-myc*-deficient lens, we performed immunofluorescence for phosphorylated NuMA (pNuMA). At E17.5, in early fiber cells nuclei (bow), pNuMA is found at multiple foci, which decrease in number following differentiation, until one or a few foci are found in late fiber cell nuclei (center, Fig. 7E-F). *N-myc* inactivation did not alter the pattern of pNuMA phosphorylation (Fig. 7G-H), suggesting that *N-myc* loss did not disrupt Cdk1 activity during fiber cell terminal differentiation.

DN*Ase*IIβ is crucial for DNA cleavage during lens differentiation (Nishimoto et al., 2003). DN*Ase*IIβ protein is first detected in early fiber cells and colocalizes with lysosomes. In late fiber cells, lysosomes
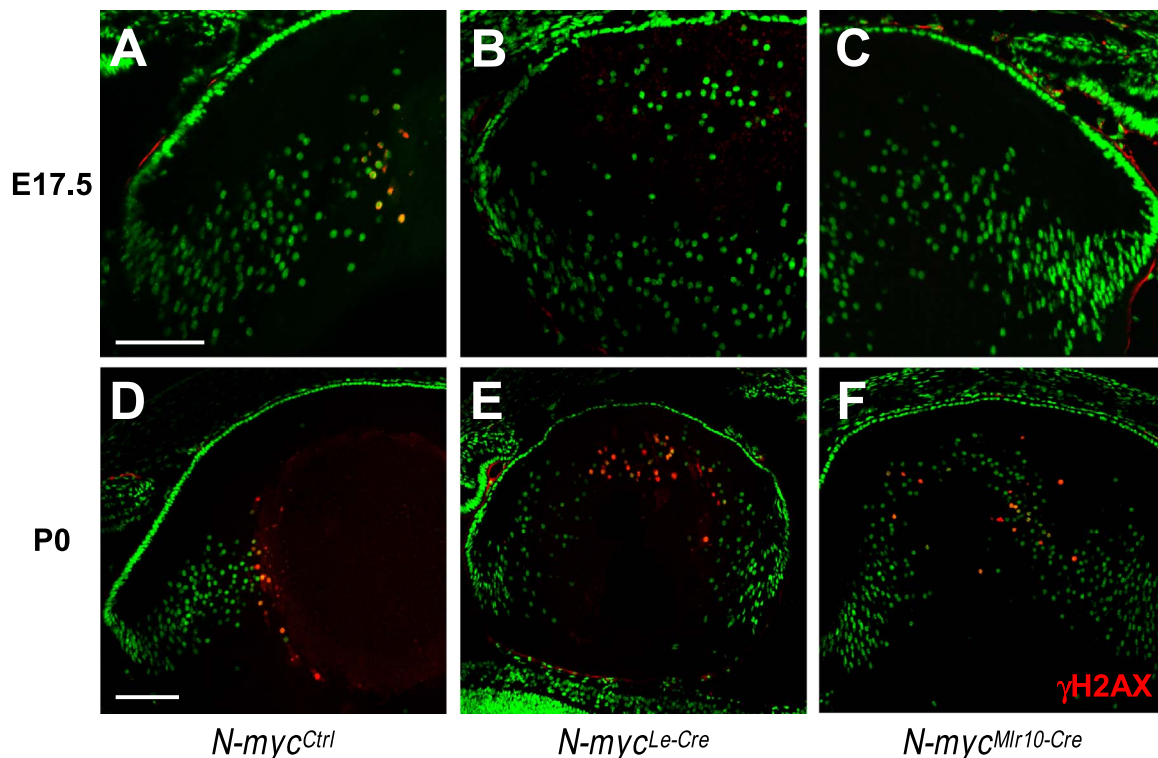

Fig. 6. Defective fiber cell denucleation in *N-myc*-deficient lenses. (A-F) Representative pictures of γH2AX immunostaining (red) in E17.5 and P0 *N-myc*[Ctrl] (A,D), *N-myc*[Le-Cre] (B,E) and *N-myc*[Mlr10-Cre] (C,F) lenses. Sytox green used for nuclei counterstaining. Scale bar: 100 μm.
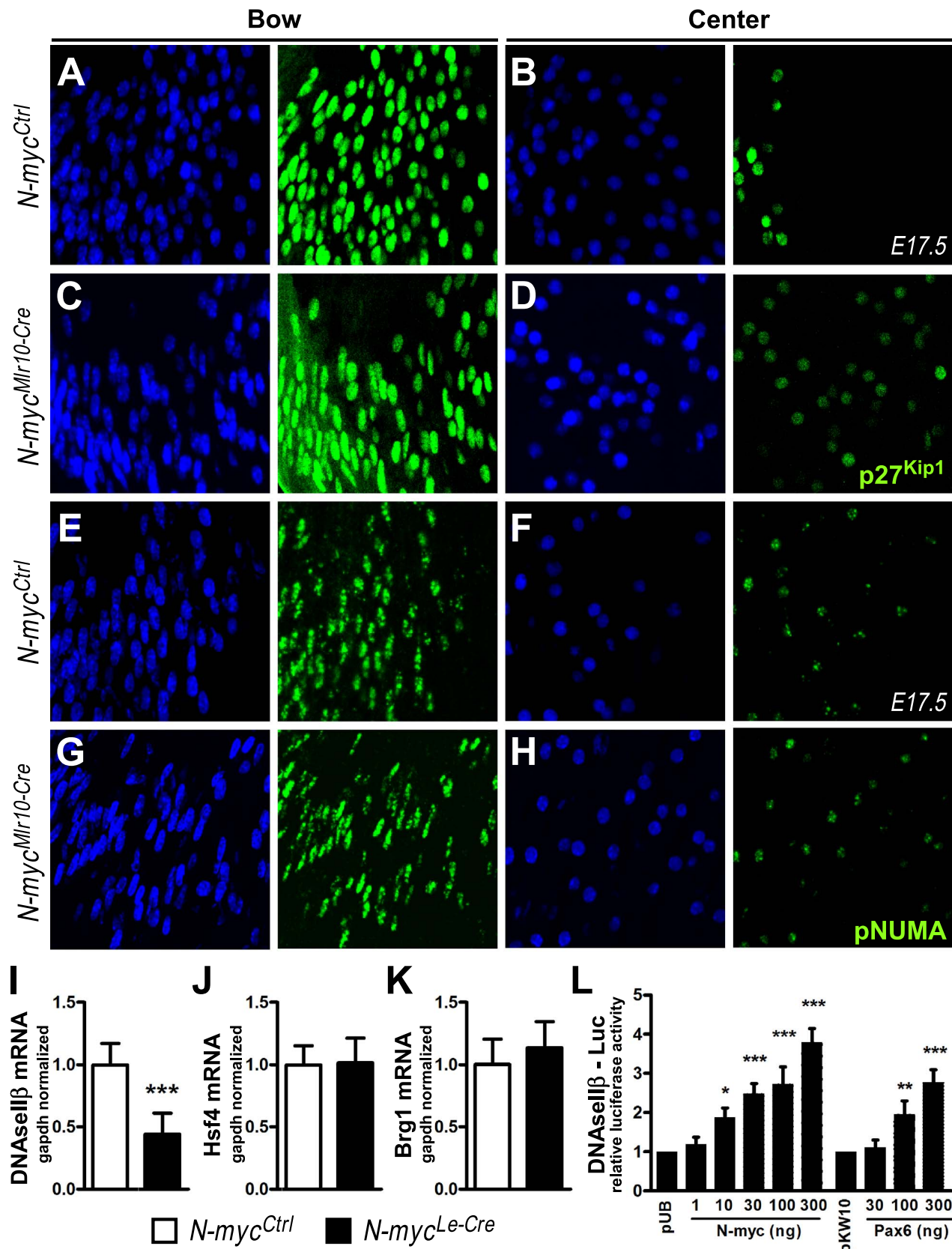
Fig. 7. Mechanisms of fiber cell denucleation in *N-myc*-deficient lenses. (A-D) Representative pictures of p27^{Kip1} immunostaining (green) in the bow (A,C) vs. center (B,D) region of the lens in *N-myc^{Ctrl}* and *N-myc$^{Mlr10-Cre}$* E17.5 mice. **(E-H)** Representative pictures of phospho-NuMA (pNuMA) immunostaining (green) in the bow (E,G) vs. center (F,H) region of the lens in *N-myc^{Ctrl}* and *N-myc$^{Mlr10-Cre}$* E17.5 mice. DAPI used for nuclear counterstaining. **(I-K)** Realtime RT-PCR analysis of *DNaseIIβ, Hsf4, and Brg1* mRNA content in P0 *N-myc^{Ctrl}* vs. *N-myc^{Le-Cre}* lenses (n = 5). **(L)** Relative fold change in the luciferase activity of DNAseIIβ-luc reporter in α-TN4 cells transfected with N-myc or Pax6 as compared to empty-vector transfected cells (n = 3). *t*-test performed in I,J and K. One-way ANOVA with Dunnett's posttest performed in L. Error bars represent S.D. *p < 0.05, **p < 0.01, ***p < 0.001. Scale bar: 25 μm.

fuse to the nuclei and release DNAseIIβ (Nakahara et al., 2007). Consistent with the RNA-Seq and RT-PCR data of *N-myc*[Mlr10-Cre] lenses (Fig. 5 and Fig. S5), *DNaseIIβ* expression was reduced in *N-myc*[Le-Cre] at P0 (Fig. 7I). Interestingly, previously characterized regulators of *DNaseIIβ* expression, Hsf4 and Brg1, (He et al., 2010) were not altered upon *N-myc* inactivation (Fig. 7J-K).

To provide evidence of whether *N-myc* could directly regulate *DNaseIIβ* transcription in the lens, we co-transfected cultured α-TN4 lens cells with *DNaseIIβ* promoter (−580 to +180) fused with luciferase reporter, and *N-myc* containing plasmid. Increasing concentrations of *N-myc* containing plasmid led to a dose-dependent increase in luciferase activity (Fig. 7L). As a positive control, co-transfection of a *Pax6* containing plasmid with the *DNaseIIβ*-luciferase construct also increased luciferase activity (Fig. 7L). Altogether, these findings indicate that the decreased expression of *DNaseIIβ* contributes to the defective denucleation following *N-myc*-inactivation, possibly through direct regulation of *DNaseIIβ* by *N-myc*.

4. Discussion

In this study, we show several evidences that the proto-oncogene *N-myc* is required for proper development of the mammalian lens. We found that inactivation of *N-myc* in distinct stages of lens development in vivo differentially impaired lens growth and caused mild microphthalmia in mice. Histological, transcriptome and biochemical assays showed that the machinery required for cellular growth is misexpressed in *N-myc*-deficient lens and that *N-myc* regulates the expression of various genes required for appropriate differentiation of lens fiber cells. More specifically, *N-myc* is required for well-timed denucleation and to high levels of *DNaseIIβ* expression. We also found that *N-myc* may directly regulate *DNaseIIβ* transcription. Based on these data, we propose that *Myc* proto-oncogenes cooperatively regulate essential functions for normal lens and eye development.

4.1. N-myc is required for lens and eye growth

A mild microphthalmia was observed when *N-myc* was inactivated from the surface ectoderm (*Le-Cre*) and from the lens vesicle (*Mlr10-Cre*), but not when inactivated in differentiating fiber cells (*Mlr39-Cre*). *N-myc* has been shown to be involved in regulation of cell proliferation, survival and growth of various embryonic tissues (Dominguez-Frutos et al., 2011; Knoepfler et al., 2002; Martins et al., 2008; Okubo et al., 2005; Wittmann et al., 2014). Unlike other tissues that require *N-myc* to develop, in the lens, *N-myc* loss did not cause severe defects in lens progenitor cells survival or proliferation during embryonic and perinatal stages of lens development.

During embryonic development, the levels of N-myc protein are relatively higher in the nucleus of fiber cells than in progenitor cells of the lens epithelium (Fig. 1D). The relatively lower levels of N-myc in proliferating cells is consistent with the lack of major defects in cell proliferation upon *N-myc* loss. It may also be that *N-myc* contributes for cell proliferation only during earlier stages of lens development (placode and vesicle stages – from E9.5 to E11.5). Alternatively, *N-myc* inactivation may cause subtle defects in cell proliferation that were bellow our detection limit. Since the lens grows substantially during embryogenesis, small variations in cell cycle dynamics during lens early development can lead to substantial effects in adult lens volume. However, in accordance with immunohistological data, global gene expression analysis did not indicate changes in the expression of genes known to regulate cell cycle and cell death in developing lens.

Importantly, most represented classes of downregulated genes after *N-myc*-inactivation belong to global control of protein synthesis. Therefore, it is possible that inefficient translation and imperfect cell growth may contribute to the tissue growth impairment of the *N-myc*-deficient lenses. Ribosomal fractionation methods were used to demonstrate that translational efficiency is affected by the loss of Myc

genes in mammary glands (Stoelzel et al., 2009). Such approaches may be adapted to study this possible role of Myc in lens cells. In addition, given that fiber cells make most of lens volume, we speculate that in *N-myc*-deficient lenses, defects in fiber cell elongation and growth may also contribute to the impairment of lens and eye growth.

Targeted deletion of *N-myc* in both retinal and lens progenitor cells led to whole eye, retina and lens growth defects (Martins et al., 2008). In contrast, inactivation of *N-myc* specifically in RPC of the retinal periphery (α-Cre) indicated that *N-myc* function in the retinoblasts is dispensable to drive lens and eye growth. Lens-specific inactivation of *N-myc* affected whole eye growth, what is probably explained by (1) the fact that the lens occupies a large fraction of eye volume and (2) the lens is important to stimulate growth of other eye structures (Coulombre and Coulombre, 1964; Coulombre and Herrmann, 1965). Therefore, we confirm previous findings that *N-myc* regulates the growth of developing ocular structures and show that *N-myc* function in the lens is required for lens growth, possibly through the regulation of multiple genes involved in cellular growth.

4.2. N-myc and c-myc play distinct roles during lens morphogenesis

Inactivation of *c-myc* in the surface ectoderm reduced cell proliferation in the embryonic lens epithelium and led to microphthalmia (Cavalheiro et al., 2014). Similarly, inactivation *N-myc* in the surface ectoderm (*Le-Cre*) or in the lens vesicle (*Mlr10-Cre*) also led to microphthalmia and microphakia. However, these phenotypes were not caused by the same cellular and molecular alterations, since *N-myc* inactivation did not affect cell proliferation levels in the lens. Conversely, as discussed bellow, c-myc loss did not interfere with lens fiber differentiation while *N-myc* loss shifted the expression of various fiber-enriched genes and perturbed denucleation.

The lens epithelium plays an important role to instruct corneal differentiation and anterior segment development (Beebe and Coats, 2000). *c-myc* inactivation in the lens resulted in defects in anterior segment differentiation (Cavalheiro et al., 2014). Normal development of the anterior segment in *N-myc*[Mlr10-Cre] mice is consistent with our proposal that only *c-myc* is required for lens epithelium homeostasis. As expected, concomitant disruption of *N-myc* and *c-myc* led to defects in anterior segment differentiation (Fig. 4), corroborating that *c-myc* and *N-myc* perform independent functions during lens development.

The increase in *c-myc* expression following *N-myc* loss in the lens placode (*Le-Cre*) or lens vesicle (*Mlr10-Cre*) led to the hypothesis that *c-myc* compensates *N-myc* loss to maintain normal cell proliferation levels. According to this, we should be able to observe a more severe growth impairment in DKO lenses in comparison to *N-myc* cKO lenses. However, we did not observe differences in lens growth between *N-myc*[Mlr10-Cre] and *N-myc;c-myc*[Mlr10-Cre] lenses (Fig. 4), indicating that *c-myc* does not compensate *N-myc* loss after lens vesicle formation. Importantly, concomitant inactivation of *N-myc* and *c-myc* in the lens placode (*N-myc;c-myc*[Le-Cre]) increased the severity of lens growth defects as compared to *N-myc* cKO (*N-myc*[Le-Cre]). Given that *c-myc* loss in *N-myc*-deficient lens vesicle did not impair lens growth in a relevant manner, it is likely that after the lens vesicle stage, these genes play independent roles. Therefore, even though no compensation occurs after lens vesicle stage, *c-myc* could display compensatory activities between lens placode and lens vesicle stages. However, one must interpret the Le-Cre results with caution, due to possible phenotypic interactions with Cre-induced phenotypes. In addition, an accumulation of cells in the vitreous chamber of *N-myc*[Le-Cre] and *N-myc;c-myc*[Le-Cre] was observed at E13.5. This may be the result of non-autonomous effects that may also contribute to the more severe phenotype of Le-Cre lenses. Further studies are necessary to better understand how *Myc* proto-oncogenes cooperate to regulate complex cellular process during ocular organogenesis.

4.3. N-myc is required for the appropriate timing of lens fiber cells terminal differentiation

In addition to promote cell cycle exit, in the lens, p27[Kip1] is important to inhibit Cdk1 activity during fiber cell generation (Rowan et al., 2016). Later, during fiber cell differentiation, p27[Kip1] degradation allows Cdk1 activity in late fiber cells. Although recent evidence suggests that Skp2 ubiquitin-ligase activity stimulates p27[Kip1] degradation in the lens (Shi et al., 2015), the mechanisms of p27[Kip1] depletion are not fully understood. *Myc* is a well-known repressor of p27[Kip1] during development, both through direct transcriptional repression and indirectly via activation of Skp2 transcription (Bretones et al., 2011; Yang et al., 2001). Defective fiber cell denucleation caused by *N-myc* loss was associated with delayed elimination of p27[Kip1] protein in late fiber cells (Fig. 7). However, it remains to be determined whether *N-myc*-mediated regulation of p27[Kip1] in lens fiber cells is direct or indirect. Interestingly, the observed reminiscence of p27[Kip1] in the absence of *N-myc* was not sufficient to prevent Cdk1 activity in late fiber nuclei. NuMA, a known Cdk1 target that is not phosphorylated in Cdk1-deficient lenses (Chaffee et al., 2014), was normally phosphorylated in late fiber cell nuclei of *N-myc*-deficient lenses.

Our RNA-Seq analysis revealed that various genes with known functions in the lens fiber cells are deregulated after *N-myc* inactivation. Indeed, our integrated analysis of the RNA-Seq data in the context of normal lens expression patterns (*iSyTE*), presence of *N-myc*-binding motif in DEGs and molecular interaction data from the String database shows that *N-myc* controls a network of genes in lens development. It identifies potential direct targets of *N-myc* and further informs on its function as a positive and negative regulator of gene expression in the lens. However, the finding that the defects in denucleation of fiber cells are transient (in P7 the *N-myc*-deficient lenses presents an OFZ) indicates that, although with some delay, the lens has mechanisms that compensate *N-myc* loss and promote fiber cell terminal differentiation, forming a transparent, functional lens (Fig. 2).

The molecular mechanisms of organelle degradation during lens development are not fully understood. Important advances on the comprehension of denucleation were achieved, however genetic interactions and posttranslational regulation needs better characterization (Chaffee et al., 2014; Rowan et al., 2016). Here, we described that *N-myc* loss interfered with the normal onset of nuclear degradation during fiber cell differentiation. *N-myc*-deficient lenses showed a delayed DNA breakdown (Figs. 2 and 6) that was associated with decreased expression of *DNaseIIβ* (Figs. 5 and 7). In addition, luciferase assays revealed that the *DNaseIIβ* promoter is modulated by *N-myc* in lens-derived cells. Interestingly, the expression of other transcriptional regulators of *DNaseIIβ* expression in the lens (Pax6, Hsf4, Brg1, Snf2h and Prox1) (Audette et al., 2016; He et al., 2016, 2010) was not altered in *N-myc*-deficient lenses (Figs. 5, 7 and S5). Altogether, these findings indicate that *N-myc* contributes to transcriptional activation of *DNaseIIβ* in the lens.

We propose that the main roles of *N-myc* during fiber cell differentiation are: (1) to stimulate transcription of genes involved in basal cellular processes and this might influence overall lens growth, and (2) to activate the expression of specific fiber cell genes, such as *DNaseIIβ*, what collaborates to trigger denucleation in an appropriate timing. The results presented here contribute to understand *Myc* functions during eye organogenesis and might help future research efforts towards understanding how developing tissues coordinate growth with cellular differentiation and its implications for lens regenerative biology.

Summary statement

Lens-specific inactivation of Myc proto-oncogenes reveals that *N-myc* regulates the proper timing of fiber cell differentiation and that c-myc and N-myc coordinately regulate eye morphogenesis.

Appendix A. Supporting information

Supplementary data associated with this article can be found in the online version at http://doi:10.1016/j.ydbio.2017.07.002.

References

de Alboran, I.M., O'Hagan, R.C., Gartner, F., Malynn, B., Davidson, L., Rickert, R., Rajewsky, K., DePinho, R.A., Alt, F.W., 2001. Analysis of C-MYC function in normal cells via conditional gene-targeted mutation. Immunity 14, 45–55.

Anand, D., Agrawal, S., Siddam, A., Motohashi, H., Yamamoto, M., Lachke, S.A., 2015. An integrative approach to analyze microarray datasets for prioritization of genes relevant to lens biology and disease. Genom. Data 5, 223–227.

Anders, S., Pyl, P.T., Huber, W., 2015. HTSeq – a Python framework to work with high-throughput sequencing data. Bioinformatics 31, 166–169.

Ashery-Padan, R., Marquardt, T., Zhou, X., Gruss, P., 2000. Pax6 activity in the lens primordium is required for lens formation and for correct placement of a single retina in the eye. Genes Dev. 14, 2701–2711.

Audette, D.S., Anand, D., So, T., Rubenstein, T.B., Lachke, S.A., Lovicu, F.J., Duncan, M.K., 2016. Prox1 and fibroblast growth factor receptors form a novel regulatory loop controlling lens fiber differentiation and gene expression. Development 143, 318–328.

Bassnett, S., 2009. On the mechanism of organelle degradation in the vertebrate lens. Exp. Eye Res. 88, 133–139.

Beebe, D.C., Coats, J.M., 2000. The lens organizes the anterior segment: specification of neural crest cell differentiation in the avian eye. Dev. Biol. 220, 424–431.

Beltran, H., 2014. The N-myc oncogene: maximizing its targets, regulation, and therapeutic potential. Mol. Cancer Res. 12, 815–822.

Berwanger, B., Hartmann, O., Bergmann, E., Bernard, S., Nielsen, D., Krause, M., Kartal, A., Flynn, D., Wiedemeyer, R., Schwab, M., Schafer, H., Christiansen, H., Eilers, M., 2002. Loss of a FYN-regulated differentiation and growth arrest pathway in advanced stage neuroblastoma. Cancer Cell 2, 377–386.

Bretones, G., Acosta, J.C., Caraballo, J.M., Ferrandiz, N., Gomez-Casares, M.T., Albajar, M., Blanco, R., Ruiz, P., Hung, W.C., Albero, M.P., Perez-Roger, I., Leon, J., 2011. SKP2 oncogene is a direct MYC target gene and MYC down-regulates p27(KIP1) through SKP2 in human leukemia cells. J. Biol. Chem. 286, 9815–9825.

Cavalheiro, G.R., Matos-Rodrigues, G.E., Gomes, A.L., Rodrigues, P.M., Martins, R.A., 2014. c-Myc regulates cell proliferation during lens development. PLoS One 9, e87182.

Chaffee, B.R., Shang, F., Chang, M.L., Clement, T.M., Eddy, E.M., Wagner, B.D., Nakahara, M., Nagata, S., Robinson, M.L., Taylor, A., 2014. Nuclear removal during terminal lens fiber cell differentiation requires CDK1 activity: appropriating mitosis-related nuclear disassembly. Development 141, 3388–3398.

Charron, J., Malynn, B.A., Fisher, P., Stewart, V., Jeannotte, L., Goff, S.P., Robertson, E.J., Alt, F.W., 1992. Embryonic lethality in mice homozygous for a targeted disruption of the N-myc gene. Genes Dev. 6, 2248–2257.

Coulombre, A.J., Coulombre, J.L., 1964. Lens development. I. Role of the lens in eye growth. J. Exp. Zool. 156, 39–47.

Coulombre, A.J., Herrmann, H., 1965. Lens development. 3. Relationship between the growth of the lens and the growth of the outer eye coat. Exp. Eye Res. 4, 302–311.

Cvekl, A., Ashery-Padan, R., 2014. The cellular and molecular mechanisms of vertebrate lens development. Development 141, 4432–4447.

Dardenne, E., Beltran, H., Benelli, M., Gayvert, K., Berger, A., Puca, L., Cyrta, J., Sboner, A., Noorzad, Z., MacDonald, T., Cheung, C., Yuen, K.S., Gao, D., Chen, Y., Eilers, M., Mosquera, J.M., Robinson, B.D., Elemento, O., Rubin, M.A., Demichelis, F., Rickman, D.S., 2016. N-Myc induces an EZH2-mediated transcriptional program driving neuroendocrine prostate cancer. Cancer Cell 30, 563–577.

Dash, S., Dang, C.A., Beebe, D.C., Lachke, S.A., 2015. Deficiency of the RNA binding protein caprin2 causes lens defects and features of Peters anomaly. Dev. Dyn. 244, 1313–1327.

Dominguez-Frutos, E., Lopez-Hernandez, I., Vendrell, V., Neves, J., Gallozzi, M., Gutsche, K., Quintana, L., Sharpe, J., Knoepfler, P.S., Eisenman, R.N., Trumpp, A., Giraldez, F., Schimmang, T., 2011. N-myc controls proliferation, morphogenesis, and patterning of the inner ear. J. Neurosci. 31, 7178–7189.

Eilers, M., Eisenman, R.N., 2008. Myc's broad reach. Genes Dev. 22, 2755–2766.

Gokhin, D.S., Nowak, R.B., Kim, N.E., Arnett, E.E., Chen, A.C., Sah, R.L., Clark, J.I., Fowler, V.M., 2012. Tmod1 and CP49 synergize to control the fiber cell geometry, transparency, and mechanical stiffness of the mouse lens. PLoS One 7, e48734.

Harmelink, C., Peng, Y., DeBenedittis, P., Chen, H., Shou, W., Jiao, K., 2013. Myocardial Mycn is essential for mouse ventricular wall morphogenesis. Dev. Biol. 373, 53–63.

Harris, L.L., Talian, J.C., Zelenka, P.S., 1992. Contrasting patterns of c-myc and N-myc expression in proliferating, quiescent, and differentiating cells of the embryonic chicken lens. Development 115, 813–820.

He, S., Pirity, M.K., Wang, W.L., Wolf, L., Chauhan, B.K., Cveklova, K., Tamm, E.R., Ashery-Padan, R., Metzger, D., Nakai, A., Chambon, P., Zavadil, J., Cvekl, A., 2010. Chromatin remodeling enzyme Brg1 is required for mouse lens fiber cell terminal differentiation and its denuclation. Epigenetics Chromatin 3, 21.

He, S., Limi, S., McGreal, R.S., Xie, Q., Brennan, L.A., Kantorow, W.L., Kokavec, J., Majumdar, R., Hou, H., Jr., Edelmann, W., Liu, W., Ashery-Padan, R., Zavadil, J., Kantorow, M., Skoultchi, A.I., Stopka, T., Cvekl, A., 2016. Chromatin remodeling enzyme Snf2h regulates embryonic lens differentiation and denuclation. Development 143, 1937–1947.

Hoang, T.V., Kumar, P.K., Sutharzan, S., Tsonis, P.A., Liang, C., Robinson, M.L., 2014. Comparative transcriptome analysis of epithelial and fiber cells in newborn mouse lenses with RNA sequencing. Mol. Vis. 20, 1491–1517.

Huang da, W., Sherman, B.T., Lempicki, R.A., 2009. Systematic and integrative analysis of large gene lists using DAVID bioinformatics resources. Nat. Protoc. 4, 44–57.

Knoepfler, P.S., Cheng, P.F., Eisenman, R.N., 2002. N-myc is essential during neurogenesis for the rapid expansion of progenitor cell populations and the inhibition of neuronal differentiation. Genes Dev. 16, 2699–2712.

Knoepfler, P.S., Zhang, X.Y., Cheng, P.F., Gafken, P.R., McMahon, S.B., Eisenman, R.N., 2006. Myc influences global chromatin structure. EMBO J. 25, 2723–2734.

Kress, T.R., Sabo, A., Amati, B., 2015. MYC: connecting selective transcriptional control to global RNA production. Nat. Rev. Cancer 15, 593–607.

Lachke, S.A., Alkuraya, F.S., Kneeland, S.C., Ohn, T., Aboukhalil, A., Howell, G.R., Saadi, I., Cavallesco, R., Yue, Y., Tsai, A.C., Nair, K.S., Cosma, M.I., Smith, R.S., Hodges, E., Alfadhli, S.M., Al-Hajeri, A., Shamseldin, H.E., Behbehani, A., Hannon, G.J., Bulyk, M.L., Drack, A.V., Anderson, P.J., John, S.W., Maas, R.L., 2011. Mutations in the RNA granule component TDRD7 cause cataract and glaucoma. Science 331, 1571–1576.

Lachke, S.A., Ho, J.W., Kryukov, G.V., O'Connell, D.J., Aboukhalil, A., Bulyk, M.L., Park, P.J., Maas, R.L., 2012. iSyTE: integrated Systems Tool for Eye gene discovery. Investig. Ophthalmol. Vis. Sci. 53, 1617–1627.

Laurenti, E., Varnum-Finney, B., Wilson, A., Ferrero, I., Blanco-Bose, W.E., Ehninger, A., Knoepfler, P.S., Cheng, P.F., MacDonald, H.R., Eisenman, R.N., Bernstein, I.D., Trumpp, A., 2008. Hematopoietic stem cell function and survival depend on c-Myc and N-Myc activity. Cell Stem Cell 3, 611–624.

Love, M.I., Huber, W., Anders, S., 2014. Moderated estimation of fold change and dispersion for RNA-seq data with DESeq. 2. Genome Biol. 15, 550.

Lovicu, F.J., McAvoy, J.W., 2005. Growth factor regulation of lens development. Dev. Biol. 280, 1–14.

Lyu, L., Whitcomb, E.A., Jiang, S., Chang, M.L., Gu, Y., Duncan, M.K., Cvekl, A., Wang, W.L., Limi, S., Reneker, L.W., Shang, F., Du, L., Taylor, A., 2016. Unfolded-protein response-associated stabilization of p27(Cdkn1b) interferes with lens fiber cell denuclation, leading to cataract. FASEB J. 30, 1087–1095.

Marquardt, T., Ashery-Padan, R., Andrejewski, N., Scardigli, R., Guillemot, F., Gruss, P., 2001. Pax6 is required for the multipotent state of retinal progenitor cells. Cell 105, 43–55.

Martins, R.A., Zindy, F., Donovan, S., Zhang, J., Pounds, S., Wey, A., Knoepfler, P.S., Eisenman, R.N., Roussel, M.F., Dyer, M.A., 2008. N-myc coordinates retinal growth with eye size during mouse development. Genes Dev. 22, 179–193.

Meyer, L.R., Zweig, A.S., Hinrichs, A.S., Karolchik, D., Kuhn, R.M., Wong, M., Sloan, C.A., Rosenbloom, K.R., Roe, G., Rhead, B., Raney, B.J., Pohl, A., Malladi, V.S., Li, C.H., Lee, B.T., Learned, K., Kirkup, V., Hsu, F., Heitner, S., Harte, R.A., Haeussler, M., Guruvadoo, L., Goldman, M., Giardine, B.M., Fujita, P.A., Dreszer, T.R., Diekhans, M., Cline, M.S., Clawson, H., Barber, G.P., Haussler, D., Kent, W.J., 2013. The UCSC Genome Browser database: extensions and updates 2013. Nucleic Acids Res. 41, D64–D69.

Meyer, N., Penn, L.Z., 2008. Reflecting on 25 years with MYC. Nat. Rev. Cancer 8, 976–990.

Nakahara, M., Nagasaka, A., Koike, M., Uchida, K., Kawane, K., Uchiyama, Y., Nagata, S., 2007. Degradation of nuclear DNA by DNase II-like acid DNase in cortical fiber cells of mouse eye lens. FEBS J. 274, 3055–3064.

Nishimoto, S., Kawane, K., Watanabe-Fukunaga, R., Fukuyama, H., Ohsawa, Y., Uchiyama, Y., Hashida, N., Ohguro, N., Tano, Y., Morimoto, T., Fukuda, Y., Nagata, S., 2003. Nuclear cataract caused by a lack of DNA degradation in the mouse eye lens. Nature 424, 1071–1074.

Okubo, T., Knoepfler, P.S., Eisenman, R.N., Hogan, B.L., 2005. Nmyc plays an essential role during lung development as a dosage-sensitive regulator of progenitor cell proliferation and differentiation. Development 132, 1363–1374.

Perng, M.D., Zhang, Q., Quinlan, R.A., 2007. Insights into the beaded filament of the eye lens. Exp. Cell Res. 313, 2180–2188.

Poschl, J., Stark, S., Neumann, P., Grobner, S., Kawauchi, D., Jones, D.T., Northcott, P.A., Lichter, P., Pfister, S.M., Kool, M., Schuller, U., 2014. Genomic and transcriptomic analyses match medulloblastoma mouse models to their human counterparts. Acta Neuropathol. 128, 123–136.

Pruitt, K.D., Tatusova, T., Brown, G.R., Maglott, D.R., 2012. NCBI Reference Sequences (RefSeq): current status, new features and genome annotation policy. Nucleic Acids Res. 40, D130–D135.

Prusky, G.T., Alam, N.M., Beekman, S., Douglas, R.M., 2004. Rapid quantification of adult and developing mouse spatial vision using a virtual optomotor system. Investig. Ophthalmol. Vis. Sci. 45, 4611–4616.

Rowan, S., Chang, M.L., Reznikov, N., Taylor, A., 2016. Disassembly of the lens fiber cell nucleus to create a clear lens: the p27 descent. Exp. Eye Res.

Sabo, A., Kress, T.R., Pelizzola, M., de Pretis, S., Gorski, M.M., Tesi, A., Morelli, M.J., Bora, P., Doni, M., Verrecchia, A., Tonelli, C., Faga, G., Bianchi, V., Ronchi, A., Low, D., Muller, H., Guccione, E., Campaner, S., Amati, B., 2014. Selective transcriptional regulation by Myc in cellular growth control and lymphomagenesis. Nature 511, 488–492.

Sawai, S., Shimono, A., Wakamatsu, Y., Palmes, C., Hanaoka, K., Kondoh, H., 1993. Defects of embryonic organogenesis resulting from targeted disruption of the N-myc gene in the mouse. Development 117, 1445–1455.

Shi, Q., Gu, S., Yu, X.S., White, T.W., Banks, E.A., Jiang, J.X., 2015. Connexin controls cell-cycle exit and cell differentiation by directly promoting cytosolic localization and degradation of E3 ligase Skp2. Dev. Cell 35, 483–496.

Stanton, B.R., Perkins, A.S., Tessarollo, L., Sassoon, D.A., Parada, L.F., 1992. Loss of N-myc function results in embryonic lethality and failure of the epithelial component of the embryo to develop. Genes Dev. 6, 2235–2247.

Stoelzle, T., Schwarb, P., Trumpp, A., Hynes, N., 2009. c-Myc affects mRNA translation, cell proliferation and progenitor cell function in the mammary gland. BMC Biol. 7, 63.

Sun, J., Rockowitz, S., Chauss, D., Wang, P., Kantorow, M., Zheng, D., Cvekl, A., 2015. Chromatin features, RNA polymerase II and the comparative expression of lens genes encoding crystallins, transcription factors, and autophagy mediators. Mol. Vis. 21, 955–973.

Trapnell, C., Pachter, L., Salzberg, S.L., 2009. TopHat: discovering splice junctions with RNA-Seq. Bioinformatics 25, 1105–1111.

Trapnell, C., Williams, B.A., Pertea, G., Mortazavi, A., Kwan, G., van Baren, M.J., Salzberg, S.L., Wold, B.J., Pachter, L., 2010. Transcript assembly and quantification by RNA-Seq reveals unannotated transcripts and isoform switching during cell differentiation. Nat. Biotechnol. 28, 511–515.

van Bokhoven, H., Celli, J., van Reeuwijk, J., Rinne, T., Glaudemans, B., van Beusekom, E., Rieu, P., Newbury-Ecob, R.A., Chiang, C., Brunner, H.G., 2005. MYCN haploinsufficiency is associated with reduced brain size and intestinal atresias in Feingold syndrome. Nat. Genet. 37, 465–467.

Wey, A., Martinez Cerdeno, V., Pleasure, D., Knoepfler, P.S., 2010. c- and N-myc regulate neural precursor cell fate, cell cycle, and metabolism to direct cerebellar development. Cerebellum 9, 537–547.

Wittmann, W., Schimmang, T., Gunhaga, L., 2014. Progressive effects of N-myc deficiency on proliferation, neurogenesis, and morphogenesis in the olfactory epithelium. Dev. Neurobiol. 74, 643–656.

Wolf, L., Gao, C.S., Gueta, K., Xie, Q., Chevallier, T., Podduturi, N.R., Sun, J., Conte, I., Zelenka, P.S., Ashery-Padan, R., Zavadil, J., Cvekl, A., 2013a. Identification and characterization of FGF2-dependent mRNA: microrna networks during lens fiber cell differentiation. G3 3, 2239–2255.

Wolf, L., Harrison, W., Huang, J., Xie, Q., Xiao, N., Sun, J., Kong, L., Lachke, S.A., Kuracha, M.R., Govindarajan, V., Brindle, P.K., Ashery-Padan, R., Beebe, D.C., Overbeek, P.A., Cvekl, A., 2013b. Histone posttranslational modifications and cell fate determination: lens induction requires the lysine acetyltransferases CBP and p300. Nucleic Acids Res. 41, 10199–10214.

Wride, M.A., 2011. Lens fibre cell differentiation and organelle loss: many paths lead to clarity. Philos. Trans. R. Soc. Lond. B Biol. Sci. 366, 1219–1233.

Yamada, S., 1990. [Expression of c-myc and N-myc in mouse embryos during craniofacial development]. Kokubyo Gakkai Zasshi 57, 83–105.

Yang, W., Shen, J., Wu, M., Arsura, M., FitzGerald, M., Suldan, Z., Kim, D.W., Hofmann, C.S., Pianetti, S., Romieu-Mourez, R., Freedman, L.P., Sonenshein, G.E., 2001. Repression of transcription of the p27(Kip1) cyclin-dependent kinase inhibitor gene by c-Myc. Oncogene 20, 1688–1702.

Yang, Y., Cvekl, A., 2005. Tissue-specific regulation of the mouse alphaA-crystallin gene in lens via recruitment of Pax6 and c-Maf to its promoter. J. Mol. Biol. 351, 453–469.

Zhao, H., Yang, Y., Rizo, C.M., Overbeek, P.A., Robinson, M.L., 2004. Insertion of a Pax6 consensus binding site into the alphaA-crystallin promoter acts as a lens epithelial cell enhancer in transgenic mice. Investig. Ophthalmol. Vis. Sci. 45, 1930–1939.

Zhao, H., Yang, T., Madakashira, B.P., Thiels, C.A., Bechtle, C.A., Garcia, C.M., Zhang, H., Yu, K., Ornitz, D.M., Beebe, D.C., Robinson, M.L., 2008. Fibroblast growth factor receptor signaling is essential for lens fiber cell differentiation. Dev. Biol. 318, 276–288.

Zhou, Z.Q., Shung, C.Y., Ota, S., Akiyama, H., Keene, D.R., Hurlin, P.J., 2011. Sequential and coordinated actions of c-Myc and N-Myc control appendicular skeletal development. PLoS One 6, e18795.